Virus Research 340 (2024) 199297

Contents lists available at ScienceDirect

Virus Research

journal homepage: www.elsevier.com/locate/virusres

The capsid protein of citrus leprosis virus C shows a nuclear distribution and interacts with the nucleolar fibrillarin protein

Mikhail Oliveira Leastro *, Vicente Pallás, Jesús Ángel Sánchez-Navarro *

Instituto de Biología Molecular y Celular de Plantas, Universitat Politècnica de Valencia-Consejo Superior de Investigaciones Científicas (CSIC), Valencia 46022, Spain

ARTICLE INFO

Keywords:
Cilevirus
CiLV-C
Capsid protein
p29
Fibrillarin
Nucleus

ABSTRACT

Brevipalpus-transmitted viruses (BTVs) have a significant negative economic impact on the citrus industry in Central and South America. Until now, only a few studies have explored the intracellular distribution and interaction of BTVs-encoded proteins with host factors, particularly for cileviruses, the main BTV responsible for the Citrus Leprosis (CL) disease. This study describes the nuclear localization of citrus leprosis virus C (CiLV-C) capsid protein (p29) and its interaction with the fibrillarin (Fib2) within the nucleolar compartment and cell cytoplasm. Our results, obtained by computer predictions and laser scanning confocal microscopy analyses, including colocalization and bimolecular fluorescence complementation (BiFC) approaches, revealed that a fraction of the p29 is localized in the nucleus and colocalizes with the Fib2 in both the nucleolus and cytosol. The nuclear localization of p29 correlated with a smaller nucleus size. Furthermore, co-immunoprecipitation (Co-IP) assays confirmed the interactions between p29 and Fib2. The implications of these findings for the functionalities of the cilevirus capsid protein are discussed.

1. Introduction

The targeting of viral particles and proteins to the nucleus has been reported in various groups of viruses that require this organelle for their infection cycle (Navarro et al., 2019; Taliansky et al., 2010). While many viruses do not necessarily require their genomes or particles to interact with the nucleus for replication, movement, or to block the antiviral defense pathway, they may require RNA-binding proteins present in this organelle for these purposes (Csorba et al., 2015; Taliansky et al., 2010; Walker and Ghildyal, 2017). Fibrillarin (Fib2) represents the major nucleolar protein localized in the nucleolus and in Cajal bodies (CBs). CBs are sub-nuclear structures known to play a significant role in RNA metabolism and the formation of ribonucleoprotein complexes (RNPs) involved in ribosome biogenesis, splicing, and transcription (Love et al., 2017). Additionally, CBs have been found to modulate various stages of virus infection (Shaw et al., 2014; Zheng et al., 2020). Fibrillarin, which is associated with ribosome biogenesis (Venema and Tollervey, 1999), is a core component of small nucleolar ribonucleoprotein particles (snoRNPs). Several viral proteins from different plant viruses have been shown to transit through the nucleolus, interacting with CBs and Fib2. These interactions were required for promoting the cell-to-cell and systemic viral transport (Kim et al., 2007a, 2007b; Li et al., 2018; Semashko et al., 2012; Zheng et al., 2015) and have also been involved in viral RNA replication and the suppression of the RNA-silencing pathway (Rajamäki and Valkonen, 2009).

Currently, citrus leprosis virus C (CiLV-C) and citrus leprosis virus C2 (CiLV-C2) are the main *Brevipalpus*-transmitted viruses (BTVs) belonging to the genus *Cilevirus*, family *Kitaviridae*. These viruses are the only accepted and most extensively studied members of the genus *Cilevirus*. The genome of cileviruses consists of two segments of positive-sense single-stranded RNA (+ssRNA) carrying 5′-cap and 3′-poly(A) tail structures (Freitas-Astua et al., 2018). For the type species CiLV-C, RNA1 encodes the polymerase precursor (RdRp) (Pascon et al., 2006) and the capsid protein (CP p29) (Leastro et al., 2018; Ortega-Rivera et al., 2023). On the other hand, RNA 2 encodes a component of the viral RNA silencing suppression (RSS) machinery (p15) (Leastro et al., 2020a), the movement protein (MP p32) (Leastro et al., 2021b, 2021c) and the putative glycoprotein (p61) and matrix protein (p24) (Kuchibhatla et al., 2014; Leastro et al., 2018).

Capsid protein (CP) of animal and plant viruses presents a structural function for the virus particles and plays a major role in most virus infection steps (Bol et al., 2008), including essential interactions with host factors during the developmental stages of the viral infection cycle (Aparicio and Pallas, 2017; Garcia and Pallas, 2015; Weber and

* Corresponding authors.
E-mail addresses: molilea@ibmcp.upv.es (M.O. Leastro), jesanche@ibmcp.upv.es (J.Á. Sánchez-Navarro).

https://doi.org/10.1016/j.virusres.2023.199297
Received 26 October 2023; Received in revised form 29 November 2023; Accepted 6 December 2023

Bujarski, 2015) and is generally accepted as a multifunctional protein (Callaway et al., 2001). Although nuclear localization has been demonstrated for the CPs of several plant RNA viruses (Anderson et al., 2012; Haupt et al., 2005; Meng and Li, 2010; Rossi et al., 2014; Zhan et al., 2016), its requirement for some function of the viral cycle has only been documented in very few examples such as viral movement (Herranz et al., 2012) or the elicitation of the host resistance response (Kang et al., 2015). Several studies performed with p29 indicate that this protein is a structural protein forming part of the viral particles (Calegario et al., 2013; Leastro et al., 2021b, 2023, 2018; Ortega-Rivera et al., 2023; Pascon et al., 2006). Based on these works, here we will refer to CiLV-C p29 as a capsid protein.

Several key findings have been reported regarding the CP of cilevirus (p29), including: i) cytoplasmatic localization in association with the endoplasmic reticulum (ER), actin filaments, and plasmodesmata; ii) intracellular traffic utilizing the ER-actin network, potentially allowing p29 to interact peripherally with cell membranes; iii) capacity to interact with cognate viral factors and movement-related proteins from dichorhavirus species; and iv) RSS activity, indicating that p29 may act as part of cilevirus counter-defense mechanism (Leastro et al., 2020a, 2020b, 2021a; Leastro et al., 2021b, 2018).

In our recent study, we reported that cileviruses MP can enter the nucleus and bind to fibrillarin (Leastro et al., 2021b). Furthermore, MP interacted with the p29 and was able to target the p29 to the plasmodesma, suggesting that these proteins may work together to ensure the viral movement and potentially other aspects of the viral infection cycle. These findings suggest a scenario in which, similar to the MP, the p29 could also undergo nuclear cycling to interact with nuclear components to facilitate various processes of virus infection, such as viral transport and/or suppression of the RNA-silencing pathway.

In this study, the nuclear and nucleolar localization of CiLV-C p29 was predicted through computer analyses and experimentally confirmed by colocalization experiments. Additionally, we revealed the *in vivo* interaction between the p29 and Fib2 using the bimolecular fluorescence complementation (BiFC) and Co-immunoprecipitation (Co-IP) assays. The BiFC assay revealed the nucleolar interaction between p29 and Fib2, as well as the putative redistribution of Fib2 from the nucleolus to the cytoplasm induced by p29.

2. Materials and methods

2.1. DNA manipulation

The *p29* gene of CiLV-C strain CRD (GenBank accession number YP_654,539.1) was obtained from total RNA extracted from symptomatic citrus leaves. The cDNA was generated by RT-PCR (Thermo Fisher Scientific, MA, USA) using an oligo(dT) primer that annealed to the 3′-poly(A) structure. Subsequently, the *p29* gene was amplified using a specific pair primer (For 5-tcatgagtatcgtaactttcactttga-3 and Rev 5-gctagc ctgcgctgagtcggagtc-3) containing the *BspH*I and *Nhe*I restriction sites.

For subcellular localization analysis, p29 was fused at its C-terminus with the enhanced green fluorescent protein (eGFP). To do this, the *p29* gene was cloned into the pSK35S-GFP:eGFP-PoPit (Leastro et al., 2018) by exchange the *GFP* gene by that of *p29* in a construct whose expression was under the control of 35S constitutive promoter from cauliflower mosaic virus (CaMV) and the terminator from the potato proteinase inhibitor (PoPit). Finally, the expression cassette (35S-p29:eGFP-PoPit) was subcloned into the pMOG800 binary plasmid using the *Eco*RI and *Xho*I restriction sites.

For BiFC assays, p29 was fused at both its N-terminus and C-terminus with the N-terminal 154 aa of the yellow fluorescent protein (NYFP) or the C-terminal 84 aa of the YFP (CYFP). Detailed procedures for obtaining these plasmids were previously described by Leastro et al. (2015). The obtained expression cassettes (35S-NYFP:p29-PoPit, 35S-p29:NYFP-PoPit, 35S-CYFP:p29-PoPit, and 35S-p29:CYFP-PoPit) were subcloned into the pMOG800 vector as aforementioned. The BiFC binary plasmids AtFib2-NYFP and AtFib2-CYFP, the negative control NoLS construct, corresponding to a nucleolar peptide signal (RKRHAKKK) (Gomez and Pallas, 2007) fused at the C-terminus of the YFP fragments, used to evaluate interaction with fibrillarin2 (Fib2), and the constructs which contained the N-terminus or C-terminus of the YFP addressed to the cytoplasm (Ncyt) or endoplasmic reticulum (Cer) were described previously (Leastro et al., 2021b).

For *in vivo* protein-protein interaction studies conducted through Co-immunoprecipitation assays, the p29, and Fib2 (AM269909.1) were fused either at their C-termini or N-termini with the HA or the 3xMyc epitopes. All genes were amplified using specific primers where the antisense (HA) or sense (3xMyc) primers contained the corresponding epitope sequence. The resulting PCR products were introduced in the construct pSK35S-eGFP-PoPit by replacing the eGFP gene through the *Nco*I/*Nhe*I restriction sites. Subsequently, the correspondent expression cassettes were subcloned into the pMOG800 binary vector.

2.2. Intracellular protein localization, BiFC assay, and nucleus marker

To visualize the p29 subcellular localization, *Agrobacterium tumefaciens* strain C58 was transformed with the binary plasmids carrying the *p29* gene fused to eGFP. Agrobacterium cultures were grown at 28 °C in Luria-Bertani (LB) medium supplemented with rifampicin (100 mg/mL^{-1}) and kanamycin (50 mg/mL^{-1}) antibiotics for agrobacterium and plasmid selection. Next, *A. tumefaciens* cultures were infiltrated (OD_{600} = 0.5) into *N. benthamiana* leaves at 2–4 weeks old. The GFP fluorescence was observed between 48 and 72 h post-infiltration (hpi) using confocal laser scanning microscope.

To investigate the localization of the p29 with cell nuclei, simultaneous infiltrations of *N. benthamiana* leaves (2–4 weeks old) with *Agrobacterium* cultures carrying the p29:eGFP (OD_{600} = 0.5) and a nucleus marker consisting of the red fluorescent protein (RFP) fused to the nuclear localization signal of SV40 large T antigen (OD_{600} = 0.1) (Leastro et al., 2020b) were performed. The nuclei areas measured from leaves 2–4 weeks old were represented by a graph containing the average of the area in mm^2 of 40 independent nuclei from different infiltrated *N. benthamiana* leaves. The nucleus area measurements were performed using the Fiji Image J program version 2.0r.

For the BiFC assay addressed to investigate the p29 and fibrillarin interaction, the p29 carrying the NYFP or CYFP fused at the N- or C-terminus were transiently expressed with the counterpart fused to the C-terminus of the fibrillarin (Fib2-NYFP and Fib2-CYFP) or the N-terminus of NoLS (NYFP-NoLS and CYFP-NoLS) (control). All procedures for BiFC assays were conducted as previously reported by Leastro et al. (2015). The YFP fluorescence was captured at 4 days post-infiltration (dpi).

For the experiments above mentioned, four leaves per plant and three plants per construct or combination of constructs were analyzed in three independent experiments. The plants were kept at 23 °C day/18 °C night and cycles of 16 h (h) light and 8 h dark, at 70 % humidity. All confocal images were obtained after multiple visualizations of different cells and regions of the *N. benthamiana* leaves.

2.3. Co-Immunoprecipitation assay (Co-IP)

The Co-IP assay was addressed using the Pierce™ HA-Tag Magnetic IP/Co-IP Kit (Thermo Scientific, USA) following the manufacturer's instructions. All procedures for Co-IP assay were conducted as previously reported by Leastro et al. (2021b).

2.4. Western blot

The p29:eGFP expression was confirmed by Western blot on 12 % SDS-PAGE, as described previously (Leastro et al., 2018), using a monoclonal anti-GFP antibody (Thermo Fisher Scientific, Waltham, MA, USA). For Co-IP, Western blot analysis was performed using 20 μl (C+)

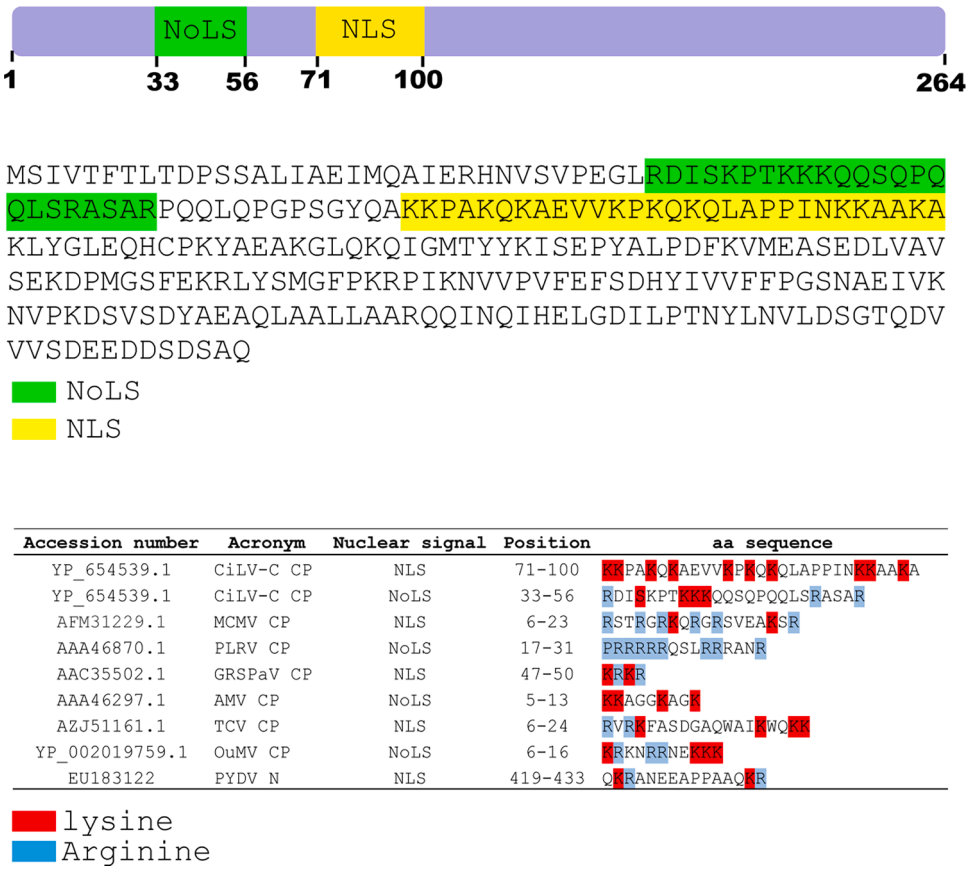

Fig. 1. Nuclear and nucleolar localization signal of the citrus leprosis virus C (CiLV-C) p29 and sequence comparison with nuclear signal domains of other viral coat proteins. Schematic representation of the CiLV-C protein highlighting the nuclear (NLS) and nucleolar (NoLS) signals. The complete amino acids sequence of CiLV-C p29 is shown. The table demonstrates NLS or NoLS sequences from CiLV-C, maize chlorotic mottle virus (MCMV), potato leafroll virus (PLRV), grapevine rupestris stem pitting-associated virus (GRSPaV), alfalfa mosaic virus (AMV), turnip crinkle virus (TCV), ourmia melon virus (OuMV), and potato yellow dwarf virus (PYDV). The lysine and arginine residues are highlighted in red and blue, respectively.

and 40 μl (IP) of proteins per line, along with two monoclonal anti-HA and anti-c-Myc antibodies (Sigma-Aldrich, Steinheim, Germany), following the manufacturer's instructions.

2.5. Confocal laser scanning microscopy

Using a laser scanning microscope Zeiss LSM 780 model, we captured the fluorescence from leaf discs of *N. benthamiana* plants. GFP was excited at 488 nm, and emission was captured at 495–520 nm. YFP was excited at 515 nm, and emission was captured at 520–560 nm. RFP was excited at 552 nm, and emission was captured at 585–610 nm. To improve the visualization of p29:eGFP expression within the nuclei, the images were acquired using the minimum laser power and gain settings necessary to eliminate the GFP signal in the cell cytoplasm (488 nm at 2.0; EGFP gain at 446; and running the laser with light control at low level). Image processing was performed using the Fiji Image J program version 2.0r.

2.6. Computer prediction analyses

Computer analyses of the deduced amino acids (a.a) sequences of the CiLV-C p29 were performed using various computational tools, including NLS mapper (http://nls-mapper.iab.keio.ac.jp/cgi-bin/NLS_Mapper_form.cgi/, accessed on 30 January 2023), NLS Stradamus (http://www.moseslab.csb.utoronto.ca/NLStradamus/, accessed on 30 January 2023), Seq NLS (http://mleg.cse.sc.edu/seqNLS/, accessed on 30 January 2023), NLSdb (https://rostlab.org/services/nlsdb/, accessed on 30 January 2023), NoD (http://www.compbio.dundee.ac.uk/www-nod/, accessed on 30 January 2023), and LocNES (http://prodata.swmed.edu/LocNES/LocNES.php/, 30 January 2023). Additionally, amino acid sequences of the orchid fleck virus (OFV) phosphoprotein (P) (BAE93580.1), known to possess a nuclear localization signal (NLS), essential for the nuclear targeting of the N-P nucleocapsid complex (Kondo et al., 2013), and the Leader peptidase (Lep) protein (WP_112,485,673.1), an integral component of bacterial membranes (Peiro et al., 2014), were included for analysis.

3. Results and discussion

3.1. Computer tools predicted NLS and NoLS signals for the p29 protein

Computer analyses using several computer tools from deduced aa of p29 protein identified a putative nuclear localization signal (NLS) for the p29 protein, encompassing residues 71–100 (data from the NLS Stradamus using a score of 0.60) (Fig. 1 and Supplementary Table 1). Additionally, a nucleolar localization signal (NoLS) was also predicted (residues 33–56) (Fig. 1 and Supplementary Table 1). However, no nuclear exportation signal (NES) was identified in the analysis (Supplementary Table 1). The robustness of the bioinformatics analysis was given by the use of positive and negative controls for NLS signals present or absent in the phosphoprotein of orchid fleck virus (OFV) and in the peptidase Lep, respectively. These computational predictions suggest that p29 has the potential to localize within the nucleus and nucleolus compartments. Most of the nuclear or nucleolar localization signals found in the CPs of plant RNA viruses are rich in arginine and lysine amino acid residues (Fig. 1). One exception is that found in the N-

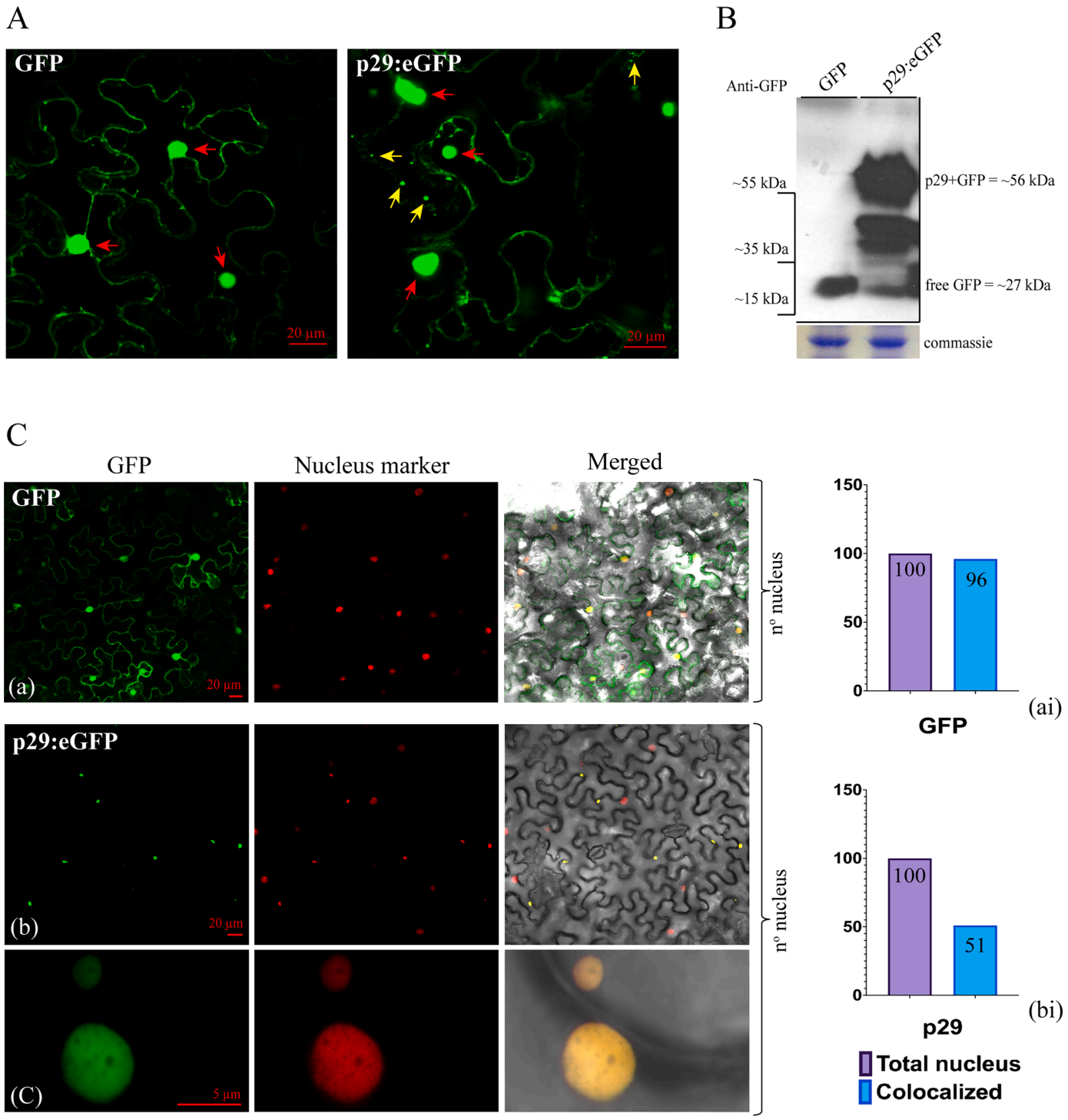

Fig. 2. Protein expression and confocal analyses of intracellular distribution and structure formation from ectopic expression of the citrus leprosis virus C (CiLV-C) p29 protein. CiLV-C p29 fused at the C-terminus of the eGFP was individually expressed and co-expressed with the mRFP nucleus marker in the epidermal cells of *Nicotiana benthamiana*. Fluorescence signals were captured 48–72 h post-infiltration (hpi) using a confocal microscope Zeiss LSM 780 model. The green (GFP), red (RFP) channels, and merged images with transmitted light are shown. **(A)** Image shows the free GFP diffuse signal distributed in the cell cytoplasm and nucleus (red arrows) and the p29:eGFP expression in punctate small (yellow arrows) and large bodies (red arrows) distributed in the cytoplasm. **(B)** Western blot of the transient accumulation of GFP (~27 kDa) and p29:eGFP (~56 kDa) proteins in *N. benthamiana* leaves. Monoclonal antibody against GFP was used to detect the free and fused GFP. The equivalent amount of leaf extract expressing the assayed proteins was analyzed. Proteins stained with Coomassie-brilliant-blue represent loading control. **(C)** Images of co-expression of the mRFP nucleus maker with free GFP **(C, a)** or p29:eGFP **(C, b). (C, c)** Image shows in higher magnification some nuclei presented in the C, b. Bars correspond to 5–20 µm. The graphs correspond to the number of nuclei accounted showing RFP fluorescence and colocalization with GFP from several leaves and plants co-infiltrated with nucleus marker plus the free GFP or the p29:eGFP.

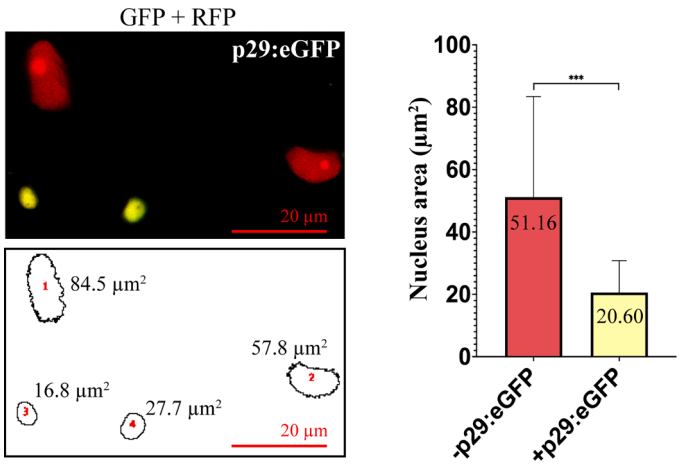

Fig. 3. Area measurement of *N. benthamiana* epidermal cell nuclei expressing p29:eGFP and/or mRFP nucleus marker. CiLV-C p29 fused at the C-terminus of the eGFP was co-expressed with the mRFP nucleus marker in the epidermal cells of *N. benthamiana*. Fluorescence signals were captured 48–72 h post-infiltration (hpi) using a confocal microscope Zeiss LSM 780 model. The green (GFP) and red (RFP) merged channels are shown. A mirror image (below) of the confocal image (above) shows the area measurement of some nuclei. The graph represents the average of the area in µm^2 of 40 independent nuclei. - p29:GFP corresponds to the nucleus expressing only RFP fluorescence (no colocalization). + p29:GFP corresponds to the nucleus expressing the GFP and RFP fluorescence (colocalization). Error bars indicate the standard deviation. Student's *t*-test and significance were set at ***$p < 0.001$.

terminal lysine-rich NoLS in the AMV CP where Lys-residues were shown to be essential for nucleolar localization of the CP (Herranz et al., 2012). The NLS identified for CiLV-C CP would be very similar to that of AMV since no Arg-residues are present in the predicted sequence (Fig. 1). In both cases, the presence of Lys-residues occurs together with Ala-residues whereas in other NLS/NoLS motifs the presence of Arg-residues is predominant.

3.2. The CiLV-C p29 shows a nuclear localization

The p29 was previously observed to have a cytoplasmatic localization, forming numerous inclusion bodies dispersed throughout the cell (Leastro et al., 2018). In this study, we confirmed this localization pattern and the structures formed by p29. The transient expression of p29:eGFP in *N. benthamiana* leaves resulted in the formation of abundant punctate and large inclusion bodies distributed throughout the cell cytoplasm (Fig. 2A, yellow and red arrows indicate small and large inclusion bodies respectively). In contrast, the expression of free GFP resulted in a diffuse fluorescent signal distributed along the cell membrane and into the nucleus (Fig. 2A; C, a). The expression of the p29:eGFP was confirmed by Western blot analysis using an anti-GFP antibody. The results showed a higher accumulation of the protein in leaves expressing p29:eGFP compared to those expressing free GFP (Fig. 2B). This abundant accumulation of p29:eGFP in the cell cytoplasm (Fig. 2A, p29:eGFP), impairs a more comprehensive visualization of other potential interaction sites of the protein within the cell using confocal microscopy. To overcome this barrier, we used a minimum confocal argon-ion laser power, and the gain was adjusted to eliminate the GFP signal in the cell cytoplasm. With this setup, only the large inclusion bodies were visible in different cells (Fig. 2C, b). Our computer-based prediction analyses suggested the potential nuclear localization of p29, as indicated by the identification of NLS and NoLS signals. To confirm these *in silico* predictions, we investigated the colocalization of the p29:eGFP large inclusion structures with the cell nuclei. Through co-expression of the p29:eGFP with a nuclear marker, we observed colocalization of the GFP signal with the nuclei of several epidermal cells of *N. benthamiana* leaves (Fig. 2C, b and c). This revealed that the structures initially thought to be large inclusion bodies were, in fact, nuclei filled with p29:eGFP. A quantitative analysis of 100 fluorescent cell nuclei showed that the nuclear localization of p29 was observed in 51 out of 100 cells (Fig. 2C, graphs).

Regardless of whether the GFP fusion is at the N- or C-terminus of CiLV-C p29, its intracellular localization remained unchanged (Leastro et al., 2018). Accordingly, in this study, we present the subcellular localization of the p29 construct with the free N-terminus.

3.3. The p29 is more associated with small nucleus

During the observation of the colocalization between p29 and the nucleus, we extensively noticed that the positive colocalization was more prominent in smaller-sized nuclei. To confirm this observation, we utilized Image J software to measure the area of 40 independent nuclei expressing either the red and green fluorescence (p29:eGFP and nucleus marker) or only the red fluorescence (nucleus marker) from different *N. benthamiana* leaves. The analysis revealed that the colocalization between the p29:eGFP and nucleus marker (RFP) was prevalent in a smaller nucleus size range of 20.6 µm^2, whereas the size range for nuclei expressing only mRFP was 51.16 µm^2 (Fig. 3). Student *t*-test shows significant differences between the means of these two groups (*p*-value < 0.01) (Fig. 3, graph).

It is well established that cell nuclei can vary in volume within a given cell type, but typically, they maintain a defined range (Mukherjee et al., 2016). In our study, we observed a higher presence of p29 in smaller-sized nuclei in the epidermal cells of *N. benthamiana*. For many viral proteins, change in subcellular localization and function can be induced by the presence of other viral factors (*i.e.* cognate viral proteins, presence of virus genome, or satellite RNAs). To better clarify the nuclear import of p29 and its prevalence in smaller nuclei, it would be interesting to investigate the dynamic of subcellular localization of the p29:eGFP in the context of virus infection. However, BTVs are restricted to the feeding site of the mite vector and apparently, they cannot spread to the distal regions of the host plants (Freitas-Astua et al., 2018). In this sense, the cilevirus movement limitation is currently challenging to study the localization of p29:eGFP in the context of virus-infected plants.

3.4. The p29 interacts with the fibrillarin, in vivo

Cilevirus MP forms an interaction complex with p29 and is also able to interact with Fib2 in the epidermal cells of *N. benthamiana* (Leastro et al., 2021b). The nuclear localization of the p29 opens the potential interaction between this protein and Fib2. To analyze this interaction by BiFC approach, leaves of *N. benthamiana* were co-infiltrated with *Agrobacterium* cultures carrying constructs of Fib2 fused with the N- or C-terminal fragments of YFP (NYFP or CYFP) and p29 constructs fused with the complementary YFP counterpart at either the N- or C-terminus. The reconstitution of the YFP fluorescent signal was observed in the nucleolar compartment of several cells (Fig. 4A, panels a and b), similar to the positive control consisting of Fib2-NYFP + Fib2-CYFP (Fig. 4A, panels c and d). No interactions were detected for negative controls (Fib2 + Ncyt, Fib2 + NoLS, p29 + Cer) (Fig. 4A, e). It is noteworthy to mention that, in addition to the nucleolar signal, the fluorescence signal derived from the p29-Fib2 interaction complex was observed also in the cytoplasm mostly associated with the cell periphery (Fig. 4A, a, white arrows). Cytoplasmic localization of Fib2 was not reported in the positive control (compare panel a with c in Fig. 4A). The cytoplasmic localization of Fib2 could suggest that the p29-Fib2 interaction occurs in the cytoplasmic compartment where they are synthesized or that the p29-Fib2 interaction leads to the redistribution of Fib2 from the nucleolus to the cell cytoplasm by p29. To confirm the p29 and Fib2 interaction, a Co-IP assay was performed. To do this, *N. benthamiana* plants were agroinfiltrated with agrobacterium cultures carrying the p29:HA and 3xMyc:Fib2 constructs and at 3 dpi, subjected to the Co-IP. A clear

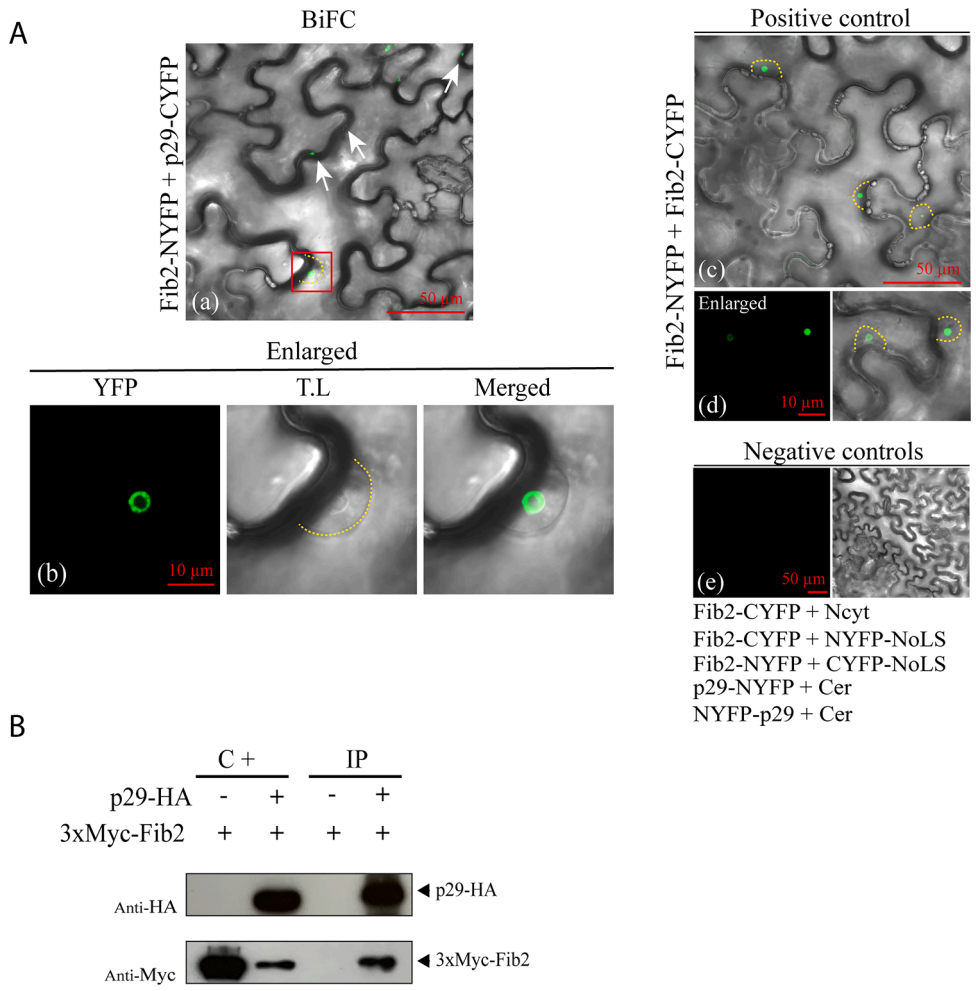

Fig. 4. Analysis of *in vivo* interaction between the capsid protein (p29) and fibrillarin. **(A)** *N. benthamiana* fibrillarin was targeted at its C-terminus with NYFP and CYFP and co-expressed with the p29 fused at its N- or C-terminus with the NYFP or CYFP. Representative protein pair combinations are indicated at the left or bottom of each image. (a-d) Image showing reconstitution of the YFP fluorescence in several nuclei. Magnification images (b and d) show the YFP signal into the nucleolus. White arrows point to the p29-Fib2 interaction complex localized in the cytoplasm and periphery of cells. Positive control (c and d) corresponds to the dimerization of the Fib2 protein by Fib2-NYFP + Fib2-CYFP co-expression. Negative control (e) corresponds to the expression of the Fib2 in combination with Ncyt and NoLS constructs and p29 in combination with the Cer construct. NoLS corresponds to a nucleolar peptide signal (RKRHAKKK) (Gomez and Pallas, 2007) fused at the C-terminus of the YFP fragments. The fluorescent signals were captured at 4 days post-infiltration (dpi). The green (GFP), transmitted light (T.L) channels, and merged images are shown in the figure. The bars indicate 10 or 50 µm. Yellow discontinuous lines highlight the nucleus compartments. The BiFC images displayed are representative of at least three independent experiments. **(B)** Co-immunoprecipitation (Co-IP) of CiLV-C p29 and Fib2. Extracts of *N. benthamiana* leaves expressing the p29:HA and 3xMyc:Fib2 constructs at 3 dpi were analyzed. The Co-IP assay was addressed using the Pierce™ HA-Tag Magnetic IP/Co-IP Kit. Myc and HA antibodies were used in the Western blots. C+, positive control (non-immunoprecipitated samples); IP, immunoprecipitated samples. The + and – signs indicate the presence or absence of the corresponding proteins in the leaf extracts.

band was observed in the immunoprecipitated extract (Fig. 4B), confirming the capacity of the cilevirus CP to interact with Fib2. Taken together, these findings further reinforce the nuclear localization of p29 and its capacity to interact with Fib2.

3.5. Could the nuclear route of cilevirus p29 and MP proteins be needed to promote the viral movement and/or suppression of RNA silencing?

Several viral proteins have been found to cycle through nucleus compartments, such as CBs and nucleolus, recruiting the fibrillarin present in these compartments for the formation of ribonucleoprotein (RNPs), essential for the short and long viral transport in the plant (Kim et al., 2007a, 2007b; Li et al., 2018; Semashko et al., 2012; Zheng et al., 2015). In the interaction between CiLV-C MP and Fib2, no redistribution of the Fib2 to the cell cytoplasm was observed (Leastro et al., 2021b). However, in this study, we reported a BiFC fluorescent signal of the p29-Fib2 complex outside the nucleolus, specifically in the cell periphery, suggesting the redistribution of Fib2 from the nucleolus to the cell cytoplasm by p29. We co-expressed the MP-Fib2 complex and p29 to investigate any potential relocation of Fib2-MP to the cytoplasm. However, we did not observe differences in the cellular localization of the MP-Fib2 complex, suggesting that other viral factors, most likely the vRNA, could be crucial for these processes (data not shown). Importantly, we cannot exclude that additional viral factor/s (likely the vRNA, other viral proteins, or both) should be necessary for this process to occur efficiently in the viral infection context. Although speculative, it is likely that the formation of a viral RNP complex containing the MP-Fib2-p29-vRNA takes place; wherein p29, together with some viral factor/s, would ensure the recruitment of Fib2 from the nucleus to the cytoplasm. On the other hand, the MP would play a role in directing the complex to the plasmodesmata at the cell periphery, given the capability of this protein to direct the p29 to these cylindrical channels (Leastro et al., 2021b), thereby facilitating the viral movement. Future studies involving silenced fibrillarin plants must be addressed to explore the

involvement of the putative Fib2-MP-p29-vRNA complex with the viral cell-to-cell and systemic transports.

The nuclear route observed for the p29 could be also required for other phases of the virus infection cycle. We recently have shown that CiLV-C p29 possesses RSS activity, suggesting its involvement in the counter-defense mechanism of the virus (Leastro et al., 2020a). Many other viral suppressors of RNA silencing (VSR) proteins also follow a nuclear route, and their nuclear localization was essential for efficient suppression of the post-transcriptional gene silencing (PTGS) pathway (Bortolamiol et al., 2007; Haas et al., 2008; Lucy et al., 2000; Zhang et al., 2006). Therefore, it is reasonable to speculate that nuclear import of p29 could also be a prerequisite for efficient suppression of silencing by CiLV-C. Nucleolus and CBs are processing centers for small RNAs, including small interfering RNAs (siRNAs) and microRNAs (miRNAs), which play crucial roles in post-transcriptional gene regulation. The Fib2, located in these compartments, is associated with snoRNPs and small nuclear RNPs (Pontes and Pikaard, 2008; Venema and Tollervey, 1999). The open question is if the p29, when associated with Fib2 in these nuclear compartments, could play a role in inhibiting the functions of small RNAs. Notably, there is a close relationship between Fib2 and VSR proteins. For instance, the RSS VPg of potato virus A (PVA) has been found into the nucleus and interacting with Fib2, where the depletion of Fib2 reduced the viral accumulation but had no effect on viral movement (Rajamäki and Valkonen, 2009). In the case of the 2b VSR protein of cucumber mosaic virus (CMV), which interacts with Fib2 in the nucleolus compartment, its RSS activity is attributed to its nuclear targeting, where it acts inhibiting AGO1 and biding to small RNAs (Gonzalez et al., 2010).

In this study, we initiate the investigation of the relationship between the capsid protein of cileviruses and the cell nucleus. Further studies are required to provide direct evidence of the putative MP-p29-Fib2 nucleus-associated complex in promoting viral movement and/or suppressing the plant antiviral defense RNA-silencing mechanism.

Funding

This work was supported by grant PID2020-115571RB-100 from the Spanish MCIN/AEI/10.13039/501100011033 granting agency and from Prometeo project CIPROM/2022/31 funded by Generalitat Valenciana.

Ethical approval

This article does not contain any studies with human participants or animals requiring ethical approval.

CRediT authorship contribution statement

Mikhail Oliveira Leastro: Conceptualization, Formal analysis, Investigation, Methodology, Writing – original draft, Writing – review & editing. **Vicente Pallás:** Writing – review & editing, Funding acquisition. **Jesús Ángel Sánchez-Navarro:** Supervision, Writing – review & editing, Funding acquisition.

Declaration of Competing Interest

The authors declare that they have no known competing financial interests or personal relationships that could have appeared to influence the work reported in this paper.

Data availability

No data was used for the research described in the article.

Acknowledgments

We are grateful to Lorena Corachán for her excellent technical support and to Elliot Watanabe Kitajima (University of Sao Paulo, Brazil) for kindly providing the CiLV-C sample used in this work.

Supplementary materials

Supplementary material associated with this article can be found, in the online version, at doi:10.1016/j.virusres.2023.199297.

References

Anderson, G., Wang, R., Bandyopadhyay, A., Goodin, M., 2012. The nucleocapsid protein of potato yellow dwarf virus: protein interactions and nuclear import mediated by a non-canonical nuclear localization signal. Front. Plant Sci. 3, 14.

Aparicio, F., Pallas, V., 2017. The coat protein of Alfalfa mosaic virus interacts and interferes with the transcriptional activity of the bHLH transcription factor ILR3 promoting salicylic acid-dependent defence signalling response. Mol. Plant Pathol. 18 (2), 173–186.

Bol, J.F., Foster, G.D., Johansen, I.E., Hong, Y., Nagy, P.D., 2008. Role of capsid proteins. Plant Virology Protocols: From Viral Sequence to Protein Function. Humana Press, Totowa, NJ, pp. 21–31.

Bortolamiol, D., Pazhouhandeh, M., Marrocco, K., Genschik, P., Ziegler-Graff, V., 2007. The polerovirus F box protein P0 targets ARGONAUTE1 to suppress RNA silencing. Curr. Biol. 17 (18), 1615–1621.

Calegario, R.F., Locali, E.C., Stach-Machado, D.R., Peroni, L.A., Caserta, R., Salaroli, R.B., Freitas-Astúa, J., Machado, M.A., Kitajima, E.W., 2013. Polyclonal Antibodies to the putative coat protein of CiLV-C (Citrus leprosis virus C) expressed in Escherichia coli: production and use in Immunodiagnosis. Trop. Plant Pathol. 38, 188–197.

Callaway, A., Giesman-Cookmeyer, D., Gillock, E.T., Sit, T.L., Lommel, S.A., 2001. The multifunctional capsid proteins of plant RNA viruses. Annu. Rev. Phytopathol. 39, 419–460.

Csorba, T., Kontra, L., Burgyán, J., 2015. viral silencing suppressors: tools forged to fine-tune host-pathogen coexistence. Virology 479-480, 85–103.

Freitas-Astua, J., Ramos-Gonzalez, P.L., Arena, G.D., Tassi, A.D., Kitajima, E.W., 2018. Brevipalpus-transmitted viruses: parallelism beyond a common vector or convergent evolution of distantly related pathogens? Curr. Opin. Virol. 33, 66–73.

Garcia, J.A., Pallas, V., 2015. Viral factors involved in plant pathogenesis. Curr. Opin. Virol. 11, 21–30.

Gomez, G., Pallas, V., 2007. A peptide derived from a single-modified viroid-RNA can be used as an "in vivo" nucleolar marker. J. Virol. Meth. 144 (1–2), 169–171.

Gonzalez, I., Martinez, L., Rakitina, D.V., Lewsey, M.G., Atencio, F.A., Llave, C., Kalinina, N.O., Carr, J.P., Palukaitis, P., Canto, T., 2010. Cucumber mosaic virus 2b protein subcellular targets and interactions: their significance to RNA silencing suppressor activity. Mol. Plant Microbe Interact. 23 (3), 294–303.

Haas, G., Azevedo, J., Moissiard, G., Geldreich, A., Himber, C., Bureau, M., Fukuhara, T., Keller, M., Voinnet, O., 2008. Nuclear import of CaMV P6 is required for infection and suppression of the RNA silencing factor DRB4. EMBO J. 27 (15), 2102–2112.

Haupt, S., Stroganova, T., Ryabov, E., Kim, S.H., Fraser, G., Duncan, G., Mayo, M.A., Barker, H., Taliansky, M., 2005. Nucleolar localization of potato leafroll virus capsid proteins. J. Gen. Virol. 86 (10), 2891–2896.

Herranz, M.C., Pallas, V., Aparicio, F., 2012. Multifunctional roles for the N-terminal basic motif of Alfalfa mosaic virus coat protein: nucleolar/cytoplasmic shuttling, modulation of RNA-binding activity, and virion formation. Mol. Plant Microbe Interact. 25 (8), 1093–1103.

Kang, S.H., Bak, A., Kim, O.K., Folimonova, S.Y., 2015. Membrane association of a nonconserved viral protein confers virus ability to extend its host range. Virology 482, 208–217.

Kim, S.H., Macfarlane, S., Kalinina, N.O., Rakitina, D.V., Ryabov, E.V., Gillespie, T., Haupt, S., Brown, J.W., Taliansky, M., 2007a. Interaction of a plant virus-encoded protein with the major nucleolar protein fibrillarin is required for systemic virus infection. Proc. Natl. Acad. Sci. U. S. A. 104 (26), 11115–11120.

Kim, S.H., Ryabov, E.V., Kalinina, N.O., Rakitina, D.V., Gillespie, T., MacFarlane, S., Haupt, S., Brown, J.W., Taliansky, M., 2007b. Cajal bodies and the nucleolus are required for a plant virus systemic infection. EMBO J. 26 (8), 2169–2179.

Kondo, H., Chiba, S., Andika, I.B., Maruyama, K., Tamada, T., Suzuki, N., 2013. Orchid fleck virus structural proteins N and P form intranuclear viroplasm-like structures in the absence of viral infection. J. Virol. 87 (13), 7423–7434.

Kuchibhatla, D.B., Sherman, W.A., Chung, B.Y., Cook, S., Schneider, G., Eisenhaber, B., Karlin, D.G., 2014. Powerful sequence similarity search methods and in-depth manual analyses can identify remote homologs in many apparently "orphan" viral proteins. J. Virol. 88 (1), 10–20.

Leastro, M.O., Castro, D.Y.O., Freitas-Astua, J., Kitajima, E.W., Pallas, V., Sanchez-Navarro, J.A., 2020a. Citrus Leprosis virus C encodes three proteins with gene silencing suppression activity. Front. Microbiol. 11, 1231.

Leastro, M.O., Freitas-Astua, J., Kitajima, E.W., Pallas, V., Sanchez-Navarro, J.A., 2020b. Dichorhaviruses movement protein and nucleoprotein form a protein complex that may be required for virus spread and interacts in vivo with viral movement-related Cilevirus proteins. Front. Microbiol. 11, 571807.

Leastro, M.O., Freitas-Astua, J., Kitajima, E.W., Pallas, V., Sanchez-Navarro, J.A., 2021a. Membrane association and topology of citrus leprosis virus C2 movement and capsid proteins. Microorganisms 9 (2), 418.
Leastro, M.O., Freitas-Astua, J., Kitajima, E.W., Pallas, V., Sanchez-Navarro, J.A., 2021b. Unravelling the involvement of cilevirus p32 protein in the viral transport. Sci. Rep. 11 (1), 2943.
Leastro, M.O., Kitajima, E.W., Pallas, V., Sanchez-Navarro, J.A., 2023. Rescue of a Cilevirus from infectious cDNA clones. Virus Res. 339, 199264.
Leastro, M.O., Kitajima, E.W., Silva, M.S., Resende, R.O., Freitas-Astua, J., 2018. Dissecting the subcellular localization, intracellular trafficking, interactions, membrane association, and topology of citrus leprosis virus C Proteins. Front. Plant Sci. 9, 1299.
Leastro, M.O., Pallas, V., Resende, R.O., Sanchez-Navarro, J.A., 2015. The movement proteins (NSm) of distinct tospoviruses peripherally associate with cellular membranes and interact with homologous and heterologous NSm and nucleocapsid proteins. Virology 478, 39–49.
Leastro, M.O., Villar-Alvarez, D., Freitas-Astua, J., Kitajima, E.W., Pallas, V., Sanchez-Navarro, J.A., 2021c. Spontaneous mutation in the movement protein of citrus leprosis virus C2, in a heterologous virus infection context, increases cell-to-cell transport and generates fitness advantage. Viruses 13 (12), 2498.
Li, Z., Zhang, Y., Jiang, Z., Jin, X., Zhang, K., Wang, X., Han, C., Yu, J., Li, D., 2018. Hijacking of the nucleolar protein fibrillarin by TGB1 is required for cell-to-cell movement of Barley stripe mosaic virus. Mol. Plant Pathol. 19 (5), 1222–1237.
Love, A.J., Yu, C., Petukhova, N.V., Kalinina, N.O., Chen, J., Taliansky, M.E., 2017. Cajal bodies and their role in plant stress and disease responses. RNA Biol. 14 (6), 779–790.
Lucy, A.P., Guo, H.S., Li, W.X., Ding, S.W., 2000. Suppression of post-transcriptional gene silencing by a plant viral protein localized in the nucleus. EMBO J. 19 (7), 1672–1680.
Meng, B., Li, C., 2010. The capsid protein of Grapevine rupestris stem pitting-associated virus contains a typical nuclear localization signal and targets to the nucleus. Virus Res. 153 (2), 212–217.
Mukherjee, R.N., Chen, P., Levy, D.L., 2016. Recent advances in understanding nuclear size and shape. Nucleus 7 (2), 167–186.
Navarro, J.A., Sanchez-Navarro, J.A., Pallas, V., 2019. Key checkpoints in the movement of plant viruses through the host. Adv. Virus Res. 104, 1–64.
Ortega-Rivera, O.A., Beiss, V., Osota, E.O., Chan, S.K., Karan, S., Steinmetz, N.F., 2023. Production of cytoplasmic type citrus leprosis virus-like particles by plant molecular farming. Virology 578, 7–12.
Pascon, R.C., Kitajima, J.P., Breton, M.C., Assumpcao, L., Greggio, C., Zanca, A.S., Okura, V.K., Alegria, M.C., Camargo, M.E., Silva, G.G., Cardozo, J.C., Vallim, M.A., Franco, S.F., Silva, V.H., Jordao Jr., H., Oliveira, F., Giachetto, P.F., Ferrari, F., Aguilar-Vildoso, C.I., Franchiscini, F.J., Silva, J.M., Arruda, P., Ferro, J.A., Reinach, F., da Silva, A.C., 2006. The complete nucleotide sequence and genomic organization of citrus leprosis associated Virus, Cytoplasmatic type (CiLV-C). Virus Genes 32 (3), 289–298.
Peiro, A., Martinez-Gil, L., Tamborero, S., Pallas, V., Sanchez-Navarro, J.A., Mingarro, I., 2014. The tobacco mosaic virus movement protein associates with but does not integrate into biological membranes. J. Virol. 88 (5), 3016–3026.
Pontes, O., Pikaard, C.S., 2008. siRNA and miRNA processing: new functions for Cajal bodies. Curr. Opin. Gen. Develop. 18 (2), 197–203.
Rajamäki, M.L., Valkonen, J.P.T., 2009. Control of nuclear and nucleolar localization of nuclear inclusion protein a of picorna-like Potato virus A in nicotiana species. Plant Cell 21 (8), 2485–2502.
Rossi, M., Genre, A., Turina, M., 2014. Genetic dissection of a putative nucleolar localization signal in the coat protein of ourmia melon virus. Arch. Virol. 159 (5), 1187–1192.
Semashko, M.A., Gonzalez, I., Shaw, J., Leonova, O.G., Popenko, V.I., Taliansky, M.E., Canto, T., Kalinina, N.O., 2012. The extreme N-terminal domain of a hordeivirus TGB1 movement protein mediates its localization to the nucleolus and interaction with fibrillarin. Biochimie 94 (5), 1180–1188.
Shaw, J., Love, A.J., Makarova, S.S., Kalinina, N.O., Harrison, B.D., Taliansky, M.E., 2014. Coilin, the signature protein of Cajal bodies, differentially modulates the interactions of plants with viruses in widely different taxa. Nucleus 5 (1), 85–94.
Taliansky, M.E., Brown, J.W., Rajamaki, M.L., Valkonen, J.P., Kalinina, N.O., 2010. Involvement of the plant nucleolus in virus and viroid infections: parallels with animal pathosystems. Adv. Virus Res. 77, 119–158.
Venema, J., Tollervey, D., 1999. Ribosome synthesis in Saccharomyces cerevisiae. Annu. Rev. Genet. 33, 261–311.
Walker, E.J., Ghildyal, R., 2017. Editorial: viral Interactions with the Nucleus. Front. Microbiol. 8 (951).
Weber, P.H., Bujarski, J.J., 2015. Multiple functions of capsid proteins in (+) stranded RNA viruses during plant-virus interactions. Virus Res. 196, 140–149.
Zhan, B., Lang, F., Zhou, T., Fan, Z., 2016. Nuclear import of Maize chlorotic mottle virus capsid protein is mediated by importin-α. Eur. J. Plant Pathol. 146 (4), 881–892.
Zhang, X., Yuan, Y.R., Pei, Y., Lin, S.S., Tuschl, T., Patel, D.J., Chua, N.H., 2006. Cucumber mosaic virus-encoded 2b suppressor inhibits Arabidopsis Argonaute1 cleavage activity to counter plant defense. Genes Develop 20 (23), 3255–3268.
Zheng, L., Du, Z., Lin, C., Mao, Q., Wu, K., Wu, J., Wei, T., Wu, Z., Xie, L., 2015. Rice stripe tenuivirus p2 may recruit or manipulate nucleolar functions through an interaction with fibrillarin to promote virus systemic movement. Mol. Plant Pathol. 16 (9), 921–930.
Zheng, L., Hong, P., Guo, X., Li, Y., Xie, L., 2020. *Rice stripe virus* p2 colocalizes and interacts with *Arabidopsis* Cajal bodies and its domains in plant cells. BioMed Res. Int. 2020, 5182164.